

# An investigation of the synthesis of nickel aluminides through gasless combustion

K. A. PHILPOT, Z. A. MUNIR

*Division of Materials Science and Engineering, University of California, Davis, California 95616, USA*

J. B. HOLT

*Department of Chemistry and Materials Science, Lawrence Livermore National Laboratory, Livermore, California 94550, USA*

The formation of nickel aluminides by the thermal explosion mode of gasless combustion synthesis was investigated for Ni–Al powders ranging in composition from 5 to 30 at% Al. Compound formation was found to take place sequentially starting with the most aluminium-rich and ending with  $\text{AlNi}_3$  as the predominant compound in the product. Compounds formed through both solid- and liquid-state reactions, with the relative contribution of each depending on the rate of heating of the powders to the reaction temperature. The effect of the particle size of nickel on these reactions was also investigated for powders with average diameters from 14 to 58  $\mu\text{m}$ .

## 1. Introduction

Strongly exothermic reactions have been observed to sustain themselves and propagate in the form of a combustion wave until the reactants have been completely consumed. Booth [1] was the first to report such observations and to lay out the mathematical foundation for what has since been referred to as the self-propagating high-temperature synthesis (SHS). Over the past two decades a multitude of investigations have been reported in which various aspects of the SHS process were examined. These investigations have included theoretical analyses of the mechanisms of combustion and experimental demonstrations of the feasibility of the process to synthesize a variety of metallic and ceramic phases, including composites [2, 3].

Of the various metallic phases investigated, aluminides have received considerable attention. These included aluminides of such metals as nickel [4–10], copper [11–13], niobium [14], palladium [15] and zirconium [16]. Preparation of the aluminides was accomplished by two modes: combustion and thermal explosion. In the former, a powder compact containing a mixture of the reactant metals is ignited at one end and the reaction propagates through the compact in the form of a combustion front. In the latter, the powder mixture is heated in a furnace until the onset of the reaction between powders of aluminium and the other metal. It has been demonstrated that regardless of which mode is utilized, the products of the reactions are identical and the maximum reaction temperatures are nearly the same [11]. In theory the highest temperature to which the product phase is raised is the adiabatic temperature which is calculated from thermodynamic functions, including the enthalpy of formation of the product and its heat capacity [17].

The nickel–aluminium binary system contains four intermetallic “compounds”:  $\text{Al}_3\text{Ni}$ ,  $\text{Al}_3\text{Ni}_2$ ,  $\text{AlNi}$  and  $\text{AlNi}_3$ . The equiatomic phase,  $\text{AlNi}$ , has the highest heat of formation and the highest melting point with values of  $-58.79 \text{ kJ mol}^{-1}$  [18] and 1911 K [19], respectively. The adiabatic temperature of  $\text{NiAl}$  has been reported as 1923 K [8] and thus, in theory, the product of combustion will be in the liquid state. Nickel aluminides, primarily the phase  $\text{NiAl}$ , have been prepared by combustion and thermal explosion modes. Under the combustion mode it was determined that the velocity of the combustion wave and the nature of the products were influenced by the initial porosity of the compacted powder mixtures [6]. Powders which were mixed to give the composition  $\text{NiAl}$  resulting in this phase exclusively when the initial porosity was 30% but resulted in a mixture of several nickel–aluminium phases when the initial porosity was 20 to 25%. Investigations using the thermal explosion mode have focused on the exothermic effects accompanying the reactions between aluminium and nickel powders [4, 5, 7]. In these investigations the temperature of powder compacts is monitored as they are heated at a constant rate inside a furnace. Deviations from the linear (constant) rate of temperature rise are indicative of reactions between the components; the magnitude of the deviations is dependent on the extent of the reactions. The temperature at which the deviation from the linear line occurs as well as the magnitude of the ensuing temperature rise were found to be dependent on the thermal history of the samples. Samples which were previously annealed exhibited a lower temperature rise relative to those which did not undergo annealing [4].

In this paper we report the results of an investigation

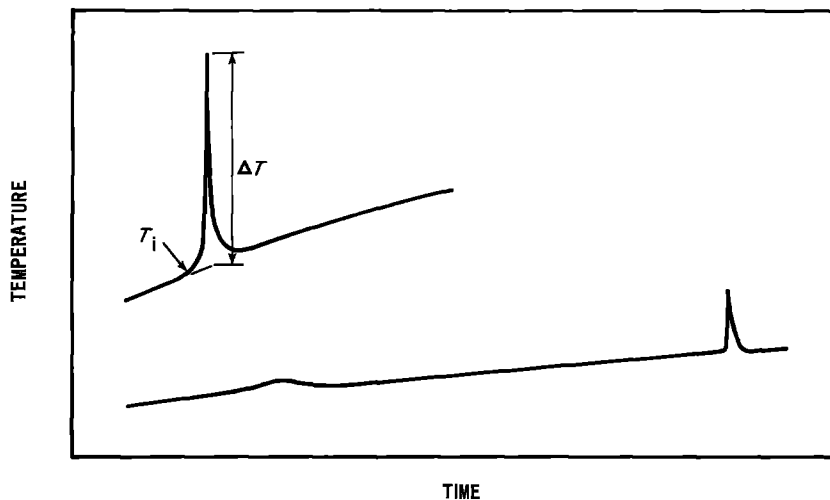


Figure 1 Schematic representation of exothermic peaks observed during the reaction between nickel and aluminium powders. 17.5 at % Al, 41  $\mu\text{m}$  nickel powder. Heating rate: upper curve 5  $\text{K min}^{-1}$ , lower curve 1  $\text{K min}^{-1}$ .

of the formation of nickel aluminides from the thermal explosion mode of gasless combustion synthesis. The objective of this study was to determine the mechanisms involved in the synthesis of these intermetallic phases and to analyse the effects of pre-combustion (diffusional) processes on the combustion process itself.

## 2. Experimental materials and methods

Powders of  $-200$  mesh nickel ( $< 74 \mu\text{m}$ ), obtained from MCB Manufacturing Chemists, Inc., (Cincinnati, Ohio, USA), and of  $-325$  mesh aluminium ( $< 44 \mu\text{m}$ ), obtained from Fisher Chemical (Pittsburgh, Pennsylvania, USA), were used as the sources for the samples prepared during this investigation. The aluminium powder was used in the as-received condition while the nickel powder was classified in size fractions with the results shown in Table I. Also included in Table I are determinations of the specific surface area and oxygen content of selected powders. The powders were hand-mixed together in a thick, acetone slurry. The mixtures were made in small batches containing powders for no more than three samples in order to minimize any chance of chemical segregation. Microscopic inspection of polished sections of various samples showed no indication of uneven mixing within the pellets. The mixture was allowed to air-dry.

Pressed compacts were formed in a stainless, cylindrical die with two plungers. The powder mixtures were compacted uniaxially at pressures ranging from 93.1 to 124 MPa to produce samples of a constant density of  $65 \pm 2\%$  of theoretical. The cylindrical samples had a diameter of 1.69 cm and heights ranging from 0.51 to 0.64 cm. The lower plunger had a small, pointed projection which formed a hole (0.49 cm deep)

in the sample bottom during pressing. The thermocouple junction was placed inside the hole for sample temperature measurement. It should be noted that in order that a constant green density be maintained in samples of varying composition, the height dimension varied. However, because the variation in height was small, it was assumed that corresponding variations in heat loss from the samples were negligible. The mass for each sample was  $7.0 \pm 0.05$  g. Samples were weighed before and after each experiment, and it was found that there was a consistent weight loss of 5 mg. This weight loss was most likely the result of volatilization of impurities and perhaps evaporation of aluminium. A metallic deposit was apparent at both ends of the water-cooled, quartz reaction tube.

A Marshall (Scott Valley, California, USA), platinum-wound, resistance-heated furnace capable of attaining 1723 K was used. Controlled, linear heating rates were obtained by using a Micricon (manufactured by Research Inc., Minneapolis, Minnesota, USA) temperature programmer which allowed for accurate, repeatable heating rates to within about  $\pm 5\%$ . All reactions were carried out in a quartz tube, placed within the furnace cavity. Experiments were run in flowing argon at 0.10 MPa (1 atm). The sample measurement thermocouple was chromel-alumel with wires of 0.254 mm diameter. Sample temperature measurements were monitored by a strip chart recorder. Examples of different time-temperature profiles observed upon reactions are shown in Fig. 1 for a sample containing 17.5 at % Al.

This experimental study involved measuring  $T_i$  (the temperature at which the sample temperature first deviated from the furnace temperature) and  $\Delta T$  (the difference between the maximum temperature measured during reaction and the baseline furnace temperature). Both parameters were measured as functions of aluminium concentration, sample heating rate and nickel powder particle size. The composition range studied was from 5 to 30 at % Al. Heating rates were varied from 0.5 to 5.0  $\text{K min}^{-1}$ . Experiments were run on samples containing  $-200$  mesh ( $< 74 \mu\text{m}$ ) nickel as well as nickel with the following four size ranges: 11 to 17, 18 to 38, 39 to 43 and 44 to 74  $\mu\text{m}$ . For practical purposes, average particle size was used for each size range when the data were plotted. As

TABLE I Powder characteristics

Material	Size fraction ( $\mu\text{m}$ )	Weight fraction (%)	Surface area ( $\text{m}^2 \text{g}^{-1}$ )	Oxygen content (wt %)
Al	$< 44$	100	0.401	$0.542 \pm 0.013$
Ni	$< 74$	100	0.108	—
Ni	44 to 73	26	0.082	$0.131 \pm 0.005$
Ni	39 to 43	23	0.086	—
Ni	18 to 38	48	0.113	$0.173 \pm 0.005$
Ni	11 to 17	3	—	—

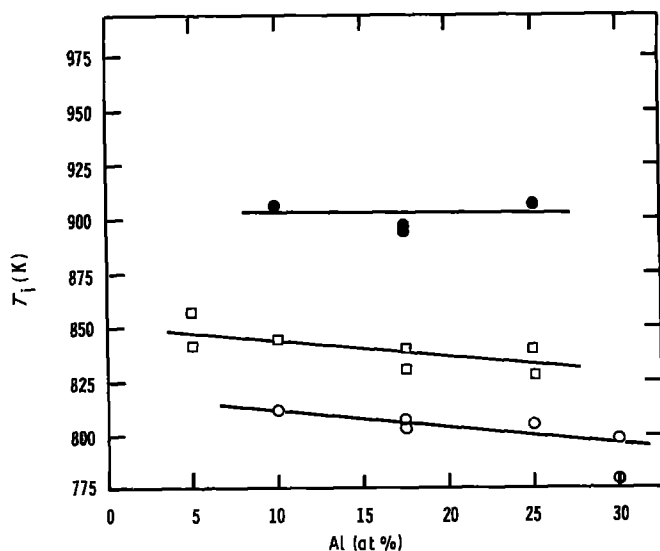


Figure 2 The dependence of  $T_i$  on aluminium content. Heating rate (○) 1 K min<sup>-1</sup>; (●) 1 K min<sup>-1</sup>, second peak; (□) 5 K min<sup>-1</sup>.

mentioned previously, the  $-325$  mesh ( $< 44 \mu\text{m}$ ) aluminium powder was used as-received for all experiments. A few experiments were also conducted to determine the influence of small additions of boron on the interaction between nickel and aluminium powders. The composition (at %) of such samples was 24.875 Al, 74.625 Ni and 0.5 B.

It is interesting to note that the samples changed in dimension during the experiment. For samples in which relatively small temperature increases were measured upon reaction ( $\Delta T < 400$  K), the sample dimensions increased, but the shape of the sample remained unchanged. In samples where large temperature increases were measured ( $\Delta T \sim 700$  K), the sample shape was changed and the dimensions increased. The top and bottom of these samples appeared to have sunk towards the centre of the sample. This change in shape was due to the presence of an aluminium-rich liquid phase which formed at the Al–Al<sub>3</sub>Ni eutectic temperature. Aside from this, the change in dimensions was a result of the formation of new phases with different lattice parameters.

### 3. Results

#### 3.1. Effect of aluminium concentration

Fig. 2 shows the dependence of  $T_i$  values on the aluminium content of powder compacts heated at 1 and 5 K min<sup>-1</sup>. The nickel powder used was  $-200$  mesh ( $< 74 \mu\text{m}$ ). When the heating rate was 5 K min<sup>-1</sup>, only one exothermic peak was observed, regardless of composition within the experimental range indicated. In contrast, when the heating rate was 1 K min<sup>-1</sup> two exothermic peaks were observed for samples with aluminium contents of up to 25 at %. Samples with a higher aluminium content, 30 at % Al, exhibited only one peak regardless of the heating rate as shown in Fig. 2. The  $T_i$  values for the first or only peak decreased with increasing aluminium content. The  $T_i$  values for the second peak, on the other hand, appear to be independent of concentration. The effect of aluminium content on the temperature rise,  $\Delta T$ , is shown in Fig. 3a for samples heated at a 5 K min<sup>-1</sup> rate and in Fig. 3b for samples heated at 1 and 2 K min<sup>-1</sup>. As stated earlier, samples heated at

5 K min<sup>-1</sup> exhibited one peak only regardless of composition and as seen in Fig. 3a the height of the peak,  $\Delta T$ , increased approximately linearly with increasing aluminium content. Also shown in Fig. 3a are results of a similar study by Naiborodenko *et al.* [7]. Agreement between the two sets of results is good. It is interesting to note that the transition from a two-peak regime to a one-peak regime is accompanied by a dramatic increase in  $\Delta T$  as seen in Fig. 3b. For example, for a heating rate of 1 K min<sup>-1</sup>, two peaks are observed up to a concentration of 25 at % Al. At this composition the  $\Delta T$  values for the first and second peaks are approximately 50 and 150 K, respectively. However, as the concentration is increased to 30 at % Al, only one peak is observed but  $\Delta T$  is increased to nearly 800 K. A similar, but less dramatic change in  $\Delta T$  is observed for the 2 K min<sup>-1</sup> rate data.

#### 3.2. Effect of heating rate

The influence of heating rate on  $T_i$  for Ni–Al samples with 10 and 25 at % Al is shown in Fig. 4. For these two compositions two peaks were observed for heating rates up to 2 K min<sup>-1</sup> and only one peak for higher rates. The  $T_i$  values, and hence the onset of the reaction between the powders, increased with increasing heating rate.

The influence of heating rate on  $\Delta T$  for samples with compositions between 5 and 30 at % Al is shown in Fig. 5. The height of the peak,  $\Delta T$ , increased with increasing heating rate, with the rate of increase being dramatic for the samples with the highest aluminium content. For the 17.5 and 25 at % Al samples the increase in  $\Delta T$  is rapid initially, but reaches an apparent asymptotic value at higher heating rates.

#### 3.3. Effect of nickel particle size

The influence of the size of the nickel particles on the reactions between nickel and aluminium was investigated using powders classified into size segments as indicated in Table I. Figs 6a to c show the dependence of  $T_i$  on particle size for compositions of 10, 17.5 and 25 at % Al, respectively. The particle size data reported in these figures are average values for each of the size classifications reported in Table I. The point

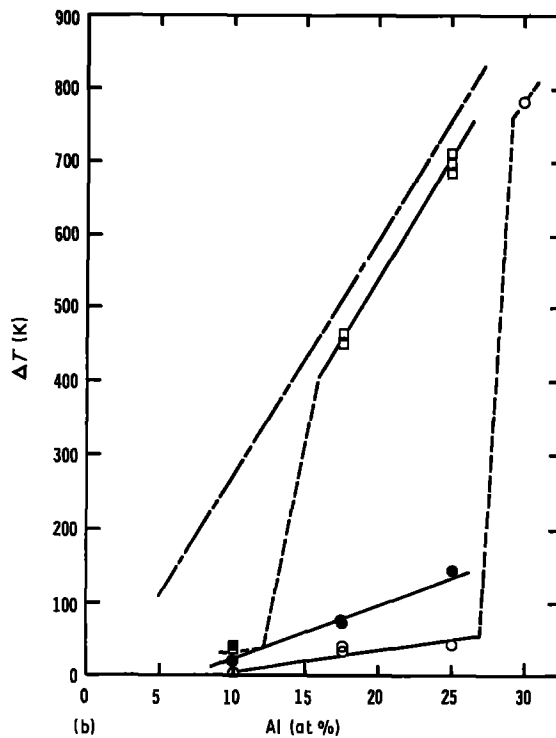
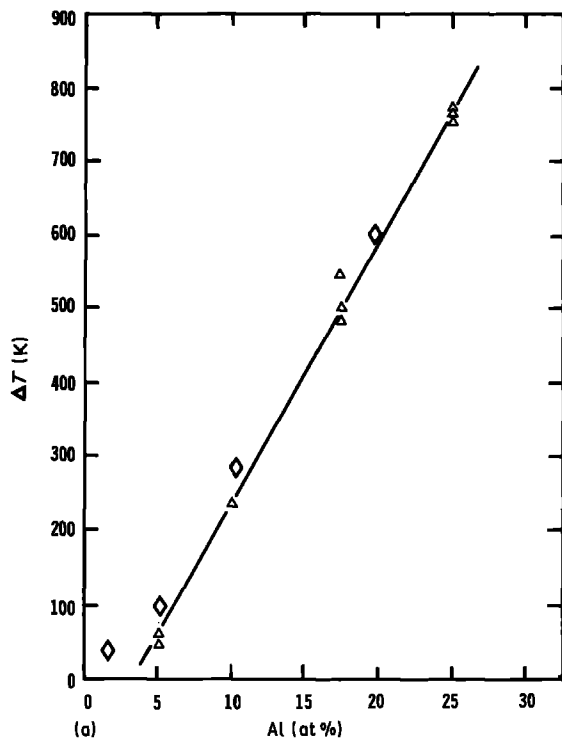


Figure 3 (a, b) The effect of composition on the temperature rise in observed exothermic peaks. Heating rate ( $\Delta$ )  $5 \text{ K min}^{-1}$ ; ( $\diamond$ )  $5 \text{ K min}^{-1}$ , from [7]; ( $\circ$ )  $1 \text{ K min}^{-1}$ ; ( $\bullet$ )  $1 \text{ K min}^{-1}$ , second peak; ( $\square$ )  $2 \text{ K min}^{-1}$ ; ( $\blacksquare$ )  $2 \text{ K min}^{-1}$ , second peak; ( $-\cdot-$ )  $5 \text{ K min}^{-1}$ .

of initiation of the reaction between the powders,  $T_i$ , generally decreases with increasing nickel particle size. This trend is true for the first and second peaks and is valid for all three compositions and all heating rates. The behaviour of powders with the largest nickel particles is interesting to examine. In contrast to the results obtained with the unclassified powder ( $< 74 \mu\text{m}$ ), two peaks were observed at a heating rate of  $5 \text{ K min}^{-1}$  when the nickel particle average size was  $58 \mu\text{m}$  as seen in Fig. 6a for the 10 at % Al samples. At a higher composition, 17.5 at % Al, only one peak is observed for powders with nickel particles of  $58 \mu\text{m}$  size heated at  $5 \text{ K min}^{-1}$  (see Fig. 6b).

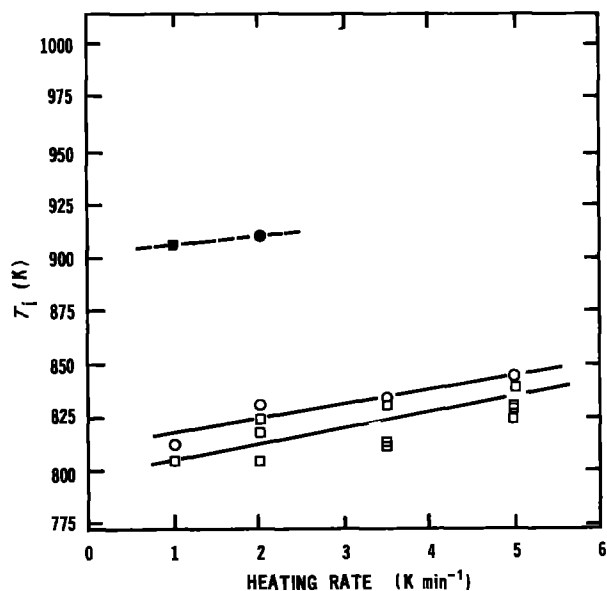


Figure 4 The dependence of  $T_i$  on heating rate for powders containing 10 and 25 at % Al. ( $\circ$ ) 10% Al; ( $\bullet$ ) 10% Al, second peak; ( $\square$ ) 25% Al; ( $\blacksquare$ ) 25% Al, second peak.

The dependence of  $\Delta T$  on particle size is depicted in Figs 7a to c for compositions of 10, 17.5 and 25 at % Al, respectively. These results show that the  $\Delta T$  values for the first and for the only peak decrease with increasing particle size. In contrast,  $\Delta T$  for the second peak, where applicable, increased with increasing nickel particle size. The transition from a one-peak

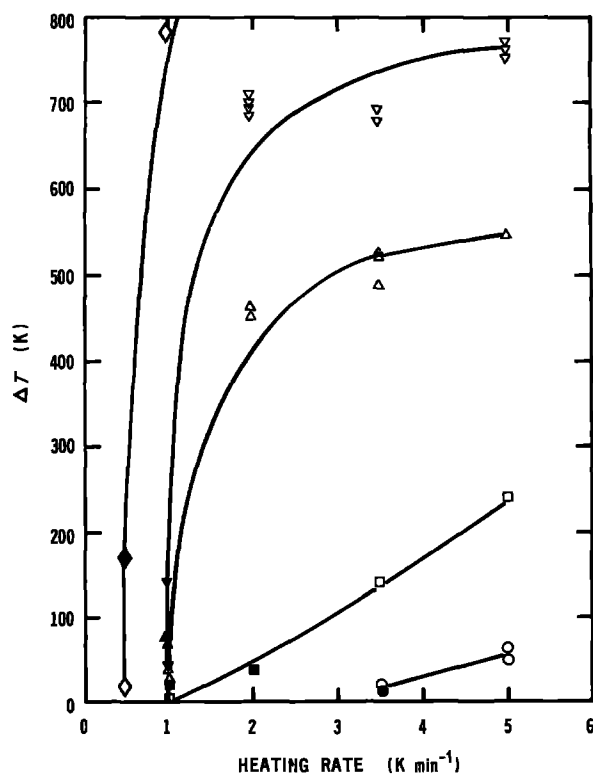


Figure 5 The effect of heating rate on the temperature rise of exothermic peaks for powders containing from 5 to 30 at % Al. Closed symbols are for second peak: ( $\circ$ ,  $\bullet$ ) 5% Al; ( $\square$ ,  $\blacksquare$ ) 19% Al; ( $\Delta$ ,  $\blacktriangle$ ) 17.5% Al; ( $\nabla$ ,  $\blacktriangledown$ ) 25% Al; ( $\diamond$ ,  $\blacklozenge$ ) 30% Al.

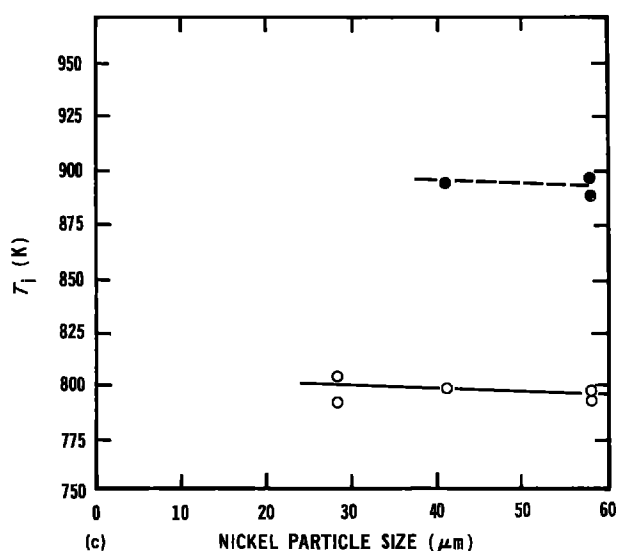
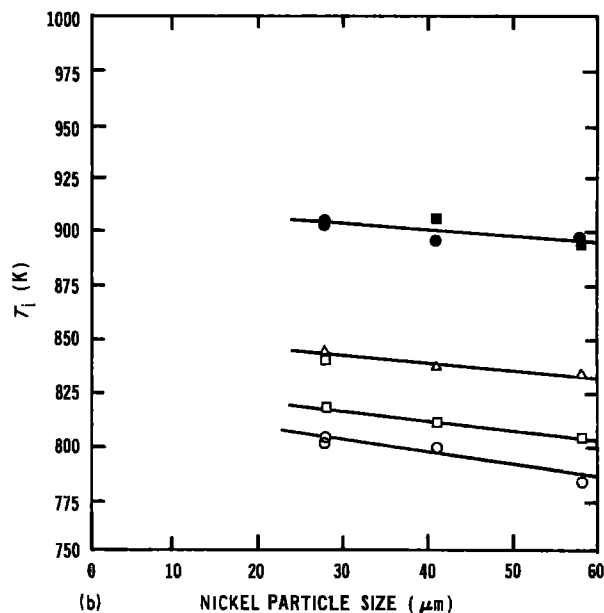
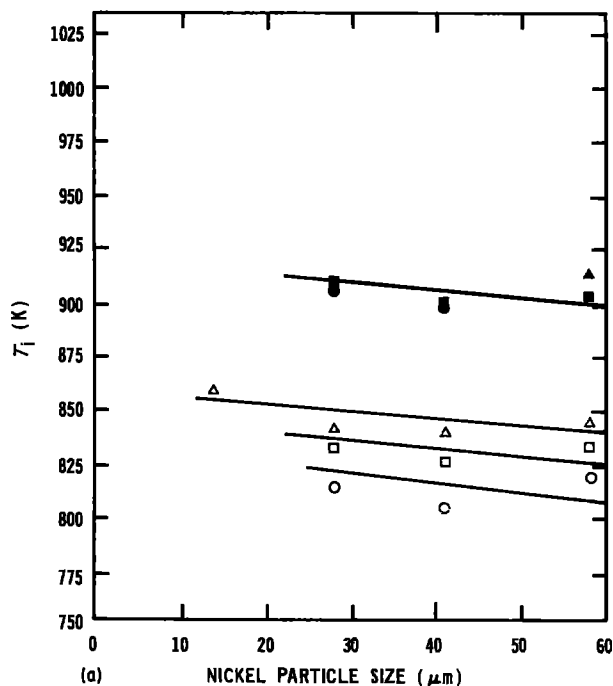


Figure 6 The dependence of  $T_i$  on nickel particle size for (a) 10 at % Al, (b) 17.5 at % Al, (c) 25 at % Al. Closed symbols are for second peak: (O, ●) 1 K min<sup>-1</sup>; (□, ■) 2 K min<sup>-1</sup>; (△, ▲) 5 K min<sup>-1</sup>.

#### 4. Discussion

The temperatures of initiation of the reactions represented by the first peak (in a two-peak system) or the only peak lie below the lowest eutectic temperature in the Al–Ni system. Thus, in both cases the reactions are initiated in the solid state. In the case of the first peak, the reaction takes place entirely between solid particles of aluminium and nickel as judged by the fact that the maximum temperature of the first peak is also lower than the eutectic temperature referred to above. In contrast, when one peak was observed the temperature rises slowly to 913 K and then abruptly after it reaches this point. In this case, therefore, the reaction is initiated in the solid state and is followed by solid–liquid interactions. Furthermore, since in all cases where two peaks were observed the highest temperature of the first peak was always lower than  $T_i$  for the second peak, we conclude that when the heat generated by the first (solid-state) reaction is sufficiently high it initiates the liquid-phase reaction and thus changes the thermal behaviour of the powders from a two-peak system to a one-peak system.

The heat generated by the solid-state reaction, as judged in this research by the  $\Delta T$  value of the first peak, is a function of composition, heating rate and nickel particle size. The temperature rise ( $\Delta T$ ) of the first peak increases with increasing aluminium content of the powders as shown in Fig. 3b, increases with increasing heating rate as shown in Fig. 5, and decreases with increasing particle size as shown in Figs 7a to c. Increasing the aluminium concentration of the powder provides for more contact between the nickel and the aluminium particles and hence an enhanced interaction resulting, as observed in this study, in a higher  $\Delta T$  for the first peak. Analogous arguments

to a two-peak behaviour as related to particle size is seen to depend on composition as well as heating rate. For example, the data shown in Fig. 7a show that for the 10 at % Al samples heated at 5 K min<sup>-1</sup>, a change from one to two peaks occurs as the average particle size increases from 41 to 58  $\mu\text{m}$ . For samples with a higher aluminium content, 17.5 at % Al, those heated at 5 K min<sup>-1</sup> exhibit one peak only over the entire particle size range shown in Fig. 7b. In this case, however, the transition occurs for the samples heated at 2 K min<sup>-1</sup> and takes place as the nickel particle size is increased from 28 to 41  $\mu\text{m}$ . For samples with a still higher composition, 25 at % Al, a transition occurs for the lowest heating rate, 1 K min<sup>-1</sup>, and takes place as the nickel particle size increases from 28 to 41  $\mu\text{m}$ . In comparing Figs 7b and c, it becomes evident that increasing the aluminium concentration results in the transition from a two-peak to a one-peak mode for the samples heated at a rate of 1 K min<sup>-1</sup>.

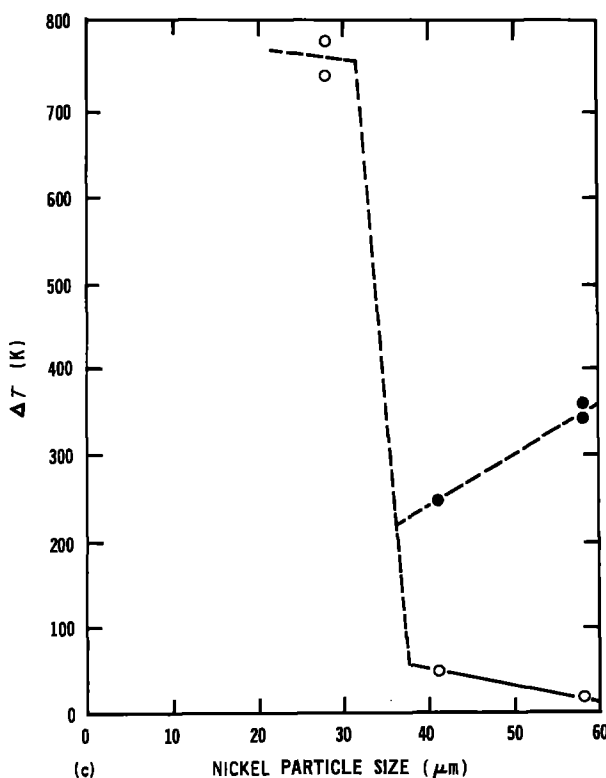
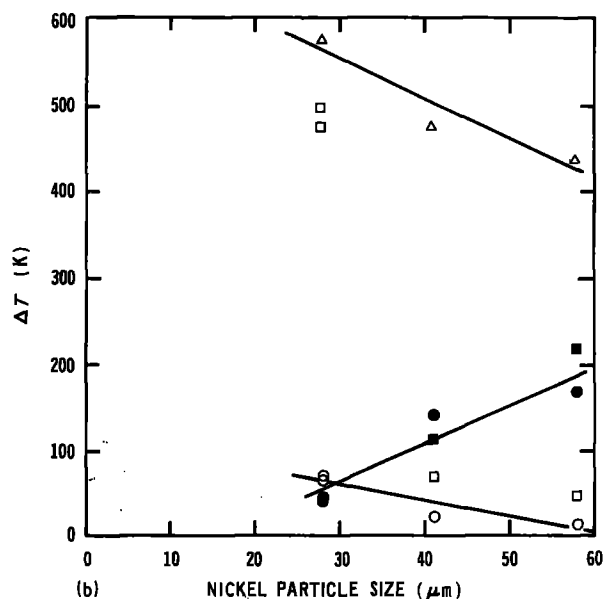
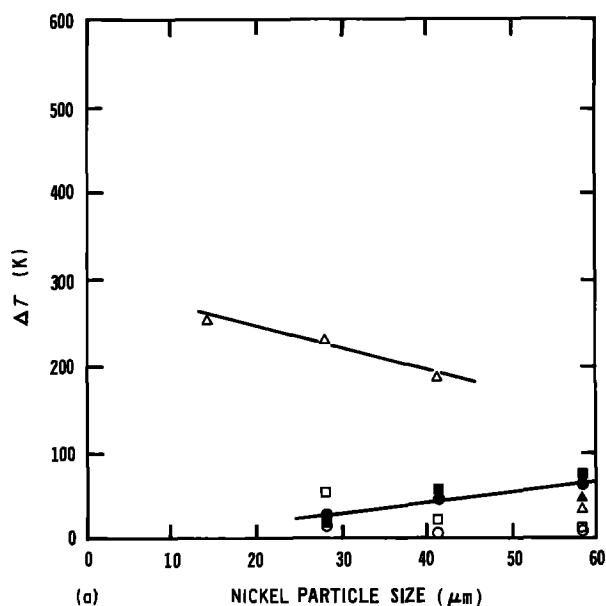


Figure 7 The dependence of  $\Delta T$  on nickel particle size for (a) 10 at % Al, (b) 17.5 at % Al, (c) 25 at % Al. Closed symbols are for second peak: (○, ●) 1 K min<sup>-1</sup>; (□, ■) 2 K min<sup>-1</sup>; (△, ▲) 5 K min<sup>-1</sup>.

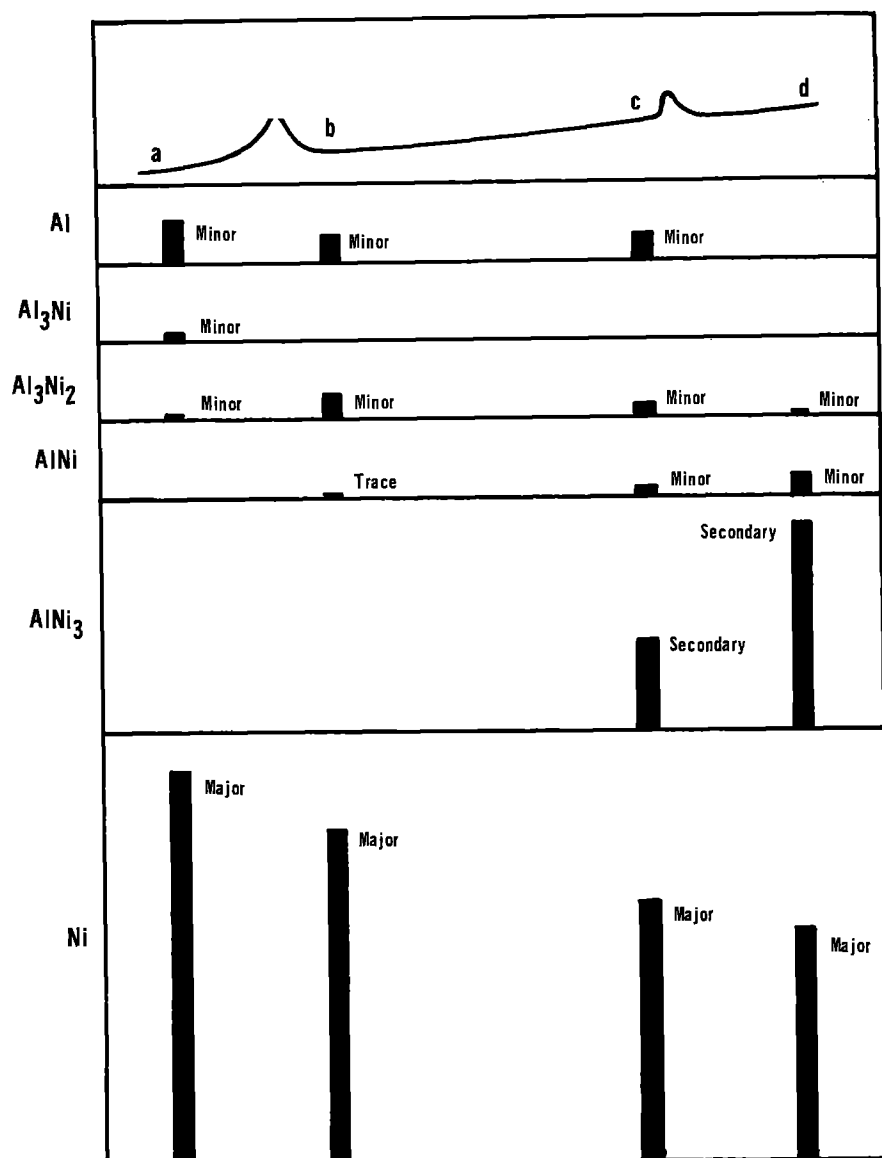
can be presented to explain the observed dependence of  $\Delta T$  on the size of the nickel particles; in this case, however, the increase in surface area is an important factor. The dependence of  $\Delta T$  on heating rate, however, cannot be clearly evaluated without a determination of the composition of the powders at different stages of reactions, as will be discussed below.

Samples containing 17.5 at % Al were used to determine the nature of the interactions between aluminium and nickel powders as they are heated through the first peak. Three samples were used. The first sample, with an average nickel particle size of 28  $\mu\text{m}$ , was heated at 1 K min<sup>-1</sup>, the second sample, with an average nickel particle size of 58  $\mu\text{m}$ , was heated at the same rate, and the third sample, with an average nickel particle size of 58  $\mu\text{m}$ , was heated at a rate of 2 K min<sup>-1</sup>. Under these experimental con-

ditions, these samples exhibited two peaks. X-ray analyses were performed on these samples after they had been heated through the first peak and the results were compared to those obtained from identical samples which were heated up to  $T_i$  of the first peak and then quenched. In all samples heated to  $T_i$  of the first peak, small amounts of  $\text{Al}_3\text{Ni}$  and  $\text{Al}_3\text{Ni}_2$  were detected; however, the major X-ray peaks observed were those for nickel and aluminium. The amounts of these two "compounds" were larger in the sample with the 28  $\mu\text{m}$  particle size than in the sample with the 58  $\mu\text{m}$  particle size. However, no differences in the amounts of these phases could be discerned between the samples heated at 1 K min<sup>-1</sup> and those heated at 2 K min<sup>-1</sup>. Thus, although not indicated by an exothermic peak, limited solid-state reactions take place prior to  $T_i$  of the first peak. X-ray analyses of samples which had gone through the first peak showed the presence of  $\text{Al}_3\text{Ni}_2$  with a trace of  $\text{AlNi}_3$  and perhaps  $\text{AlNi}$ . No  $\text{Al}_3\text{Ni}$  was detected. Thus, the reactions associated with the first peak involve the formation of  $\text{Al}_3\text{Ni}_2$  from the direct interaction between the elements and from the reaction of nickel with  $\text{Al}_3\text{Ni}$  to give  $\text{Al}_3\text{Ni}_2$ . As in the case for samples heated up to  $T_i$  of the first peak, nickel and aluminium lines were the major peaks in the X-ray results of the samples which were heated through the first peak. Also, as in the case of those samples heated up to  $T_i$ , samples with the small particle size (28  $\mu\text{m}$ ) resulted in the largest amount of  $\text{Al}_3\text{Ni}_2$  formed, and again no difference could be detected between samples of equal particle size heated at the two rates indicated above.

The observations just described showed no difference in the amounts of phases resulting from heating samples through the first peak at 1 K min<sup>-1</sup> and at 2 K min<sup>-1</sup>. This observation, we believe, is a consequence of the limitation of the X-ray method in identifying differences between quantities near the lower

Figure 8 Representation of relative amounts of phases present at various stages of reaction between nickel and aluminium powders. 17.5 at % Al, heating rate  $1 \text{ K min}^{-1}$ ,  $28 \mu\text{m}$  nickel powder.



limits of detection. Lower heating rates are expected to lead to the formation of larger amounts of  $\text{Al}_3\text{Ni}$  and  $\text{Al}_3\text{Ni}_2$  phases before the onset of the first peak and, consequently, to a smaller  $\Delta T$  for this peak as has been observed in this study (see Fig. 7b). Fig. 7b also shows that the  $\Delta T$  for the first peak was largest for samples with the smallest nickel particle size,  $28 \mu\text{m}$  consistent with the expectation that higher particle surface area results in greater interactions.

The observation that detectable amounts of phases can form without an associated thermal peak led us to investigate the nature of interactions along the entire course of the combustion process. For this purpose we have analysed the products of interactions between nickel and aluminium powders at four points along the reaction path. Samples with a composition of 17.5 at % Al and having a nickel particle size of  $28 \mu\text{m}$  were heated at a rate of  $1 \text{ K min}^{-1}$  to the following points and then examined by X-ray analysis: (a) just below  $T_i$  of the peak, (b) the end of the first peak, (c) just below  $T_i$  of the second peak, and (d) the end of the second peak. In all cases the samples were cooled immediately after reaching the desired temperature by turning the furnace power off and continuing the flow of the inert gas. The results of the X-ray analysis are

shown in Fig. 8 along with a schematic diagram of the temperature-time curve corresponding to the samples used. The amounts of the phases indicated in Fig. 8 are relative and are based on measurements of the areas under the most prominent X-ray peaks for the indicated elements and compounds. The results obtained from analysis of samples heated to points a and b are in agreement with those described above. Specifically, it was found that small amounts of  $\text{Al}_3\text{Ni}$  and  $\text{Al}_3\text{Ni}_2$  formed in samples heated to point a, and that the exothermic reactions giving rise to the first peak involve the formation of  $\text{Al}_3\text{Ni}_2$  from the elements and from the reaction of nickel with  $\text{Al}_3\text{Ni}$ . No  $\text{Al}_3\text{Ni}$  was detected in samples heated to point b. The conclusion that  $\text{Al}_3\text{Ni}_2$  has formed through the interaction between the elements is based on the observed decrease in the amounts of nickel and aluminium as seen in Fig. 8. Also observed at point b is a trace of  $\text{AlNi}$ .

Analysis of samples heated to point c (Fig. 8) revealed the presence of  $\text{AlNi}_3$  as the major compound with smaller amounts of  $\text{Al}_3\text{Ni}_2$  and  $\text{AlNi}$ . The amount of aluminium appears to be unchanged as the samples are heated from b to c. In contrast, the amount of nickel decreased for the corresponding

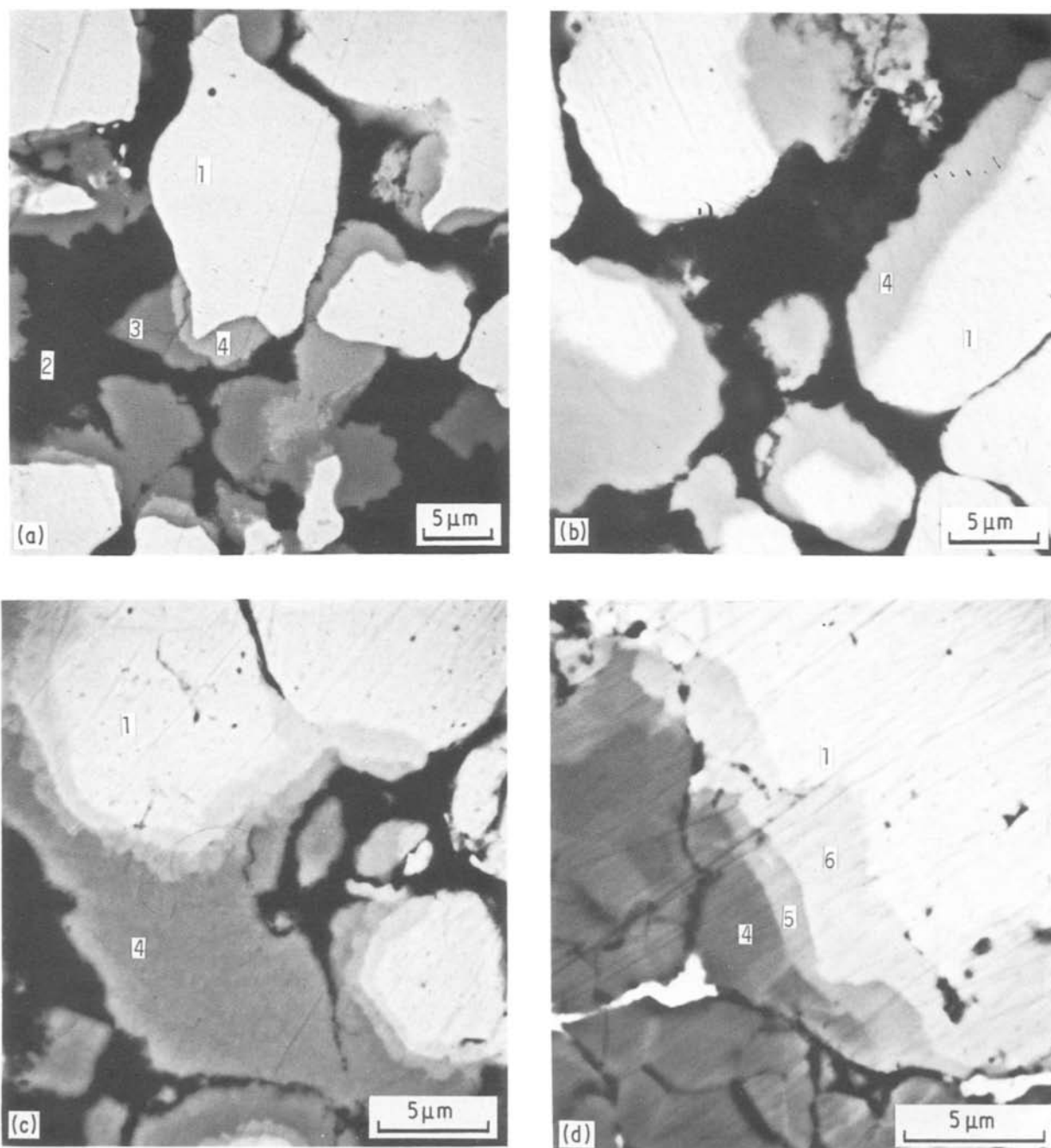


Figure 9 SEM micrographs of 17.5 at % Al powders heated at  $1 \text{ K min}^{-1}$  to (a)  $T_i$  of first peak, (b) through the first peak, (c) to  $T_i$  of second peak and (d) through the second peak. Average nickel particle size:  $28 \mu\text{m}$ . (1) Pure nickel, (2) pure aluminium, (3)  $\text{Al}_3\text{Ni}$ , (4)  $\text{Al}_3\text{Ni}_2$ .

change in thermal history. Finally, when samples were heated to point d, the primary product was  $\text{AlNi}_3$ , although minor amounts of  $\text{AlNi}$  and  $\text{Al}_3\text{Ni}_2$  were still present. It should be noted that at this point all of the aluminium has been consumed and that substantial amounts of unreacted nickel remained. These findings can be summarized by the following equations representing progressive reactions taking place at the specified segment of the thermal history:

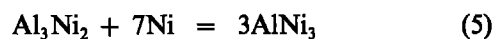
(i) Before the onset of the first peak



(ii) Through the first peak



(iii) Between the end of the first peak and the onset of the second peak



(iv) Through the second peak



These results reveal that thermal effects are related to the type of reaction as well as the amounts of product formed. For example, although significant amounts of  $\text{AlNi}_3$  formed between points b and c, no peak was observed. In contrast, a large thermal effect is observed between points c and d and as has been demonstrated by the X-ray results, the primary reaction taking place between these points is the formation of  $\text{AlNi}_3$ . In the former case,  $\text{AlNi}_3$  forms from the

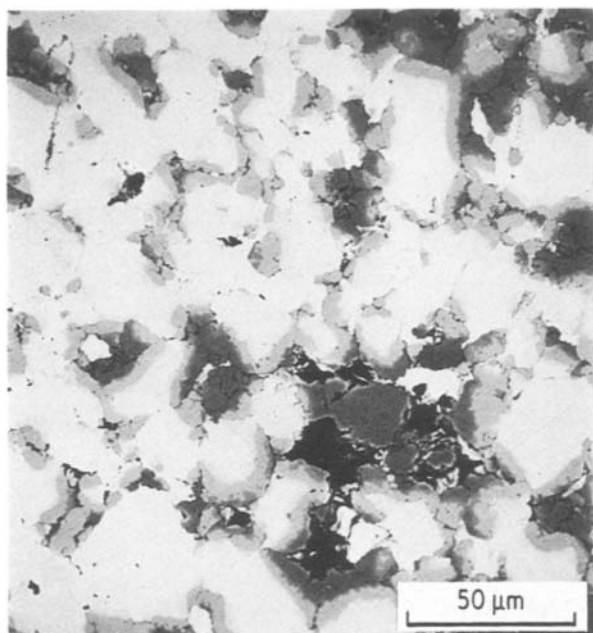


Figure 10 Lower magnification of SEM micrograph of 17.5 at % Al powders heated through the second peak.

reaction of nickel with nickel aluminides (Equations 5 and 6) and in the latter case the phase forms from the reaction between elements (Equation 7). Simple thermodynamic calculations show that the second type of reaction is more exothermic than the first. Moreover, the reaction associated with the second peak involves a liquid phase and hence is expected to be relatively rapid, giving rise to the dramatic increase in temperature.

It is significant to note that although the powders underwent partial melting at 913 K, no indication of an endothermic reaction was observed. As has been suggested previously [4], the observed abrupt rise in temperature is the consequence of the reaction between solid nickel particles and a nickel-rich aluminium liquid. The dissolution of nickel in molten aluminium has been shown to be extremely rapid [20].

Scanning electron microscope (SEM) observations on samples heated to the four points (a to d) indicated in Fig. 8 showed the formation of the products in a layered form consistent with X-ray observations. Fig. 9a is an SEM micrograph of a sample heated to point a (refer to Fig. 8). In this image from back-scattered electrons, the light area, identified by the number 1 is pure nickel and the darkest area, numbered 2, is pure aluminium. The other phases are  $\text{Al}_3\text{Ni}$  and  $\text{Al}_3\text{Ni}_2$ , identified by the numbers 3 and 4, respectively. Figs 9b to d are similar micrographs of samples heated to points b to d, respectively. The grey-coloured region (numbered 4) in Fig. 9b is  $\text{Al}_3\text{Ni}_2$ , and the narrow phase between  $\text{Al}_3\text{Ni}_2$  and nickel is probably  $\text{AlNi}$ . Fig. 9c shows layers of  $\text{AlNi}$  and  $\text{AlNi}_3$  between  $\text{Al}_3\text{Ni}_2$  (numbered 4) and nickel (numbered 1) located in the expected order of an increasing nickel content between region 4 and region 1. A similar arrangement of phases is seen in Fig. 9d where regions 5 and 6 refer to the phases  $\text{AlNi}$  and  $\text{AlNi}_3$ , respectively. The micrographs of Figs 9a to d were selected to show the presence and arrangement of the

various phases and are not necessarily indicative of their magnitude. This is clearly demonstrated by Fig. 10, which represents a lower magnification of Fig. 9d and which reveals the presence of large amounts of nickel (lightest phase) in addition to the reaction product  $\text{AlNi}_3$  (light grey phase).

In order to gain additional insight concerning the reactions involved, it is instructive to focus on the relationship between the observed thermal effects and the results of X-ray analysis. X-ray results of samples with a composition of 17.5 at % Al and with a nickel particle size of  $28\ \mu\text{m}$  showed that the amounts of the product phase,  $\text{AlNi}_3$ , were approximately equal for all heating rates. Yet samples with this composition experienced markedly different thermal treatment as can be seen from Fig. 7b. For the samples heated at  $1\ \text{K min}^{-1}$  two peaks were observed with  $\Delta T$  values for the first and second being 70 and 42 K, respectively. In contrast, samples heated at 2 and  $5\ \text{K min}^{-1}$  result in one peak with  $\Delta T$  values of 486 and 572 K, respectively. Despite the large differences in the  $\Delta T$  values, the amount of product formed was the same, as stated above. The differences in  $\Delta T$ , therefore, relate to the extent of formation of the product through liquid-phase reactions. For the samples heated at the slow rate ( $1\ \text{K min}^{-1}$ ), significant amounts of the product phase ( $\text{AlNi}_3$ ) formed through solid-state reactions as can be seen from the X-ray data depicted in Fig. 8. In this case the amount of free aluminium has been decreased, leading to a lower exothermicity of the liquid-phase reaction, i.e. a lower  $\Delta T$  as observed experimentally. For samples heated at a higher heating rate (e.g.  $5\ \text{K min}^{-1}$ ), the reverse is true with most of the product being formed through the liquid-phase reaction giving rise to a higher  $\Delta T$ .

In contrast to the samples containing 17.5 at % Al (described above), those containing higher amounts of aluminium showed a dependence of the amount of product formed on the heating rate. Samples containing 25 at % Al heated at a rate equal to or higher than  $2\ \text{K min}^{-1}$  had more  $\text{AlNi}_3$  formed than in samples heated at  $1\ \text{K min}^{-1}$ . This observation suggests that the formation of the product phase in the 17.5 at % Al samples is limited by the aluminium content, and more significantly, that the amounts of product formed are influenced by the thermal history of the sample prior to the process of combustion.

The presence of a liquid phase in powder compacts can lead to a decrease in porosity through rearrangement or sintering. Thus, we anticipate that compacts in which the reactions are primarily in the liquid phase will have lower porosities at the end of the reactions. Results obtained in this study show agreement with this anticipation. Three samples were examined: the first was a 25 at % Al sample which was heated at  $1\ \text{K min}^{-1}$ , the second sample had the same composition but was heated at  $5\ \text{K min}^{-1}$ , and the third sample had a composition of 24.875 at % Al, 74.625 at % Ni and 0.5 at % B and was heated at  $5\ \text{K min}^{-1}$ . SEM micrographs of these samples are shown in Figs 11a to c, respectively. Image analyses were performed on these SEM micrographs to give the percentage porosity values listed in Table II.

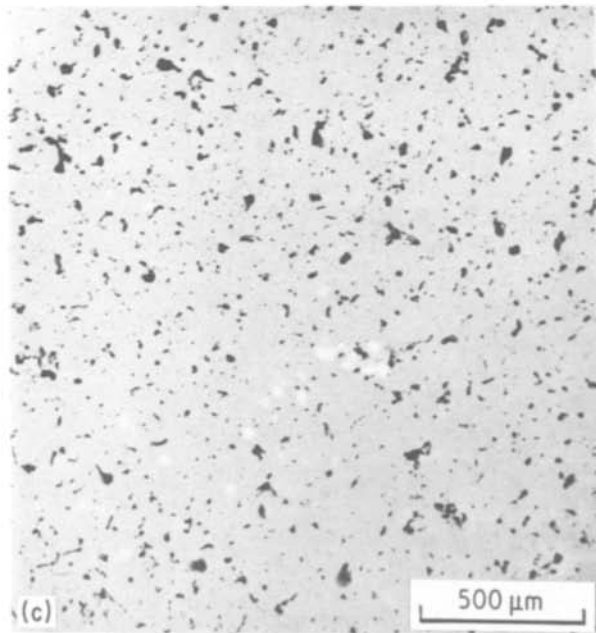
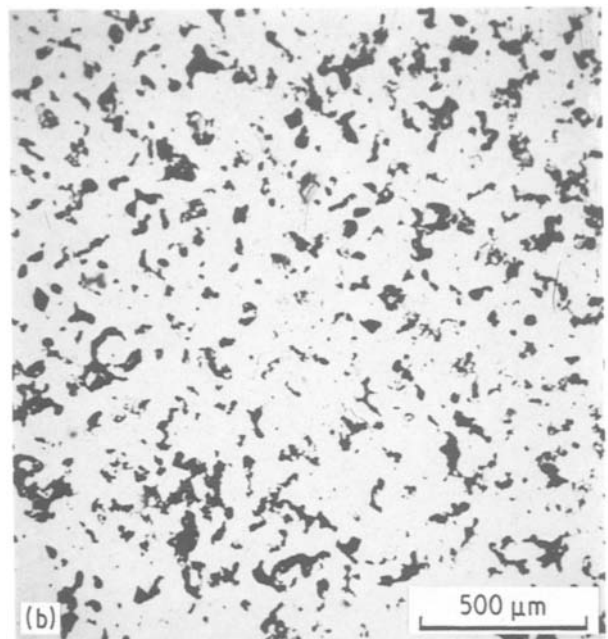
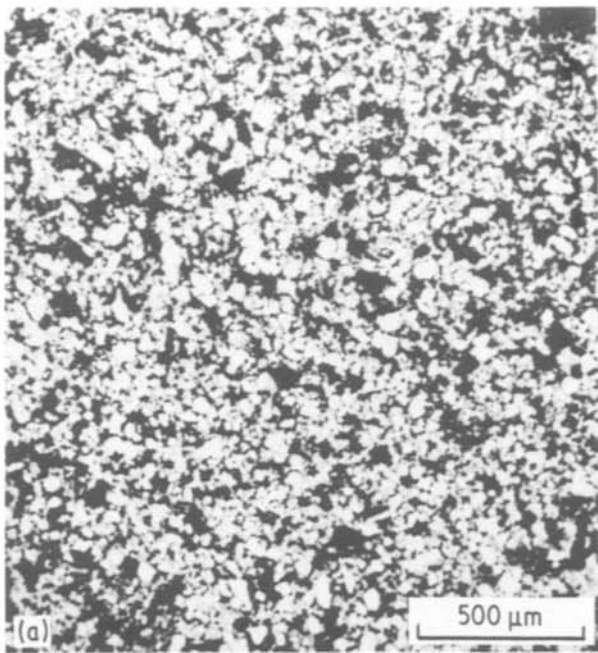


Figure 11 Porosity in 25 at % Al powders heated at (a)  $1 \text{ K min}^{-1}$  and (b)  $5 \text{ K min}^{-1}$  through the second peak. — 200 mesh nickel particles. (c) Porosity of powders with a nominal composition of 25 at % Al but containing 0.5 at % B heated at  $5 \text{ K min}^{-1}$  through the second peak. — 200 mesh nickel particles.

Consistent with stated expectations, samples in which reactions took place primarily in the liquid state had the lower porosity, as can be seen by comparing the results of the sample heated at  $1 \text{ K min}^{-1}$  with those of the sample heated at  $5 \text{ K min}^{-1}$  (Table II). The addition of small amounts of boron (0.5 at %) enhances this trend even further, resulting in a porosity of 7%. The exact role played by boron is not clearly understood in the present studies.

TABLE II Dependence of sample porosity on heating rate and boron addition

Sample composition (at % Al)	Heating rate ( $\text{K min}^{-1}$ )	Porosity (%)
25	1	28
25	5	16
"25" + 0.5 at % B	5	7

### Acknowledgement

We are grateful to the Defense Advanced Research Program Agency for the financial support of this work.

### References

1. F. BOOTH, *Trans. Faraday Soc.* **49** (1953) 272.
2. A. G. MERZHANOV, *Archiv. Combust.* **1** (1981) 23.
3. I. P. BOROVINSKAYA, G. A. VISHNIAKOVA, V. M. MASLOV and A. G. MERZHANOV, in "Combustion Processes in Chemical Technology and Metallurgy" (Moscow, 1975) p. 141.
4. Y. S. NAIBORODENKO, V. I. ITIN and K. V. SAVITSKII, *Sov. Phys. J.* **11** (1968) 19.
5. *Idem, ibid.* **11** (1968) 89.
6. Y. S. NAIBORODENKO, V. I. ITIN, A. G. MERZHANOV, I. P. BOROVINSKAYA, V. P. USHAKOV and V. P. MASLOV, *ibid.* **16** (1973) 872.
7. Y. S. NAIBORODENKO, V. I. ITIN, B. P. BELOZEROV and V. P. USHAKOV, *ibid.* **16** (1973) 1507.
8. Y. S. NAIBORODENKO and V. I. ITIN, *Comb. Explos. Shock Wave* **11** (1975) 293.
9. *Idem, ibid.* **11** (1975) 626.
10. V. M. MASLOV, I. P. BOROVINSKAYA and A. G. MORZHANOV, *ibid.* **12** (1976) 631.
11. Y. S. NAIBORODENKO, V. I. ITIN and K. V. SAVITSKII, *Sov. Powd. Metall. Ceram.* No. 7(91) (1970) 562.
12. V. I. IYIN, A. D. BRATCHIKOV and L. N. POSTNIKOVA, *ibid.* No. 5(209) (1980) 315.
13. V. I. ITIN, A. D. BRATCHIKOV and A. V. LEPINSKIKH, *Comb. Explos. Shock Wave* **17** (1981) 506.
14. V. M. MASLOV, I. P. BOROVINSKAYA and M. K. ZIATDINOV, *ibid.* **15** (1979) 41.
15. M. R. BIRNBAUM, Sandia Laboratories (Livermore, California) Report No. SAND 78-8503 (1978).
16. E. A. NEKRASOV, Y. M. MAKSIMOV and A. P. ALDUSHIN, *Comb. Explos. Shock Wave* **17** (1981) 140.
17. J. B. HOLT and Z. A. MUNIR, *J. Mater. Sci.* **21** (1986) 251.

18. R. HULTGREN, "Selected Values of Thermodynamic Properties of Metals and Alloys" (American Society for Metals, Metal Park, Ohio, 1973) p. 191.
19. M. HANSEN, "Constitution of Binary Alloys", 2nd Edn (McGraw-Hill, New York, 1958) p. 118.

20. M. M. JANSSEN and G. D. RIECK, *Trans. Met. Soc. AIME* **239** (1967) 1372.

*Received 17 February  
and accepted 28 April 1986*